

# Structural and spectroscopic properties of BaHfO<sub>3</sub>: Eu – the issue of the dopant location in the host lattice

A. Dobrowolska, E. Zych\*

University of Wrocław, Faculty of Chemistry, 14 F. Joliot – Curie, 50-383 Wrocław, Poland

\* zych@wchuwr.pl

**Keywords:** Barium hafnate, luminescence, site-selective spectroscopy, defects

**Abstract.** BaHfO<sub>3</sub>:Eu powders containing 0-10% of the dopant with respect to Hf were synthesized with the classic ceramic method at 1400°C. X-ray diffraction analysis proved that up to 10% of the Eu concentration the product is crystallographically pure and crystallizes in a cubic perovskite-type structure. Detailed structural measurements showed that the size of the unit cell decreases up to the Eu concentration of 3% and increases when the dopant content is further increased. Spectroscopic analysis gave evidence that three different symmetry sites of Eu<sup>3+</sup> exist in BaHfO<sub>3</sub>:Eu(5%) powders. It is postulated that two of them results from simple substitution of the Ba<sup>2+</sup> and Hf<sup>4+</sup> ion sites and the third one results from (Eu<sub>Hf</sub> - Eu<sub>Ba</sub>) pair formation. Only one of the sites, giving emission peaking at 595.6 nm is fully centrosymmetric, although positions of both metal ions in the host material possess inversion symmetry.

## Introduction

Barium hafnate (BaHfO<sub>3</sub>) was found to be an attractive host lattice for new X-ray phosphors [1,2,3]. Due to high effective atomic number and high density (64.58 and 8.5 g/cm<sup>3</sup>, respectively) [3] barium hafnate containing materials have distinctly higher photofraction and absorption coefficient in the range of medical X-rays [4] compared to today commercial phosphors used in planar imaging and computed tomography based on Gd<sub>2</sub>O<sub>2</sub>S (57.72, 7.34 g/cm<sup>3</sup>, respectively). Till now luminescence and radioluminescence properties of BaHfO<sub>3</sub> were studied mostly on Ce-doped compositions, which appeared to have efficient and fast decaying radioluminescence, which parameters are important for computed tomography and positron emission tomography [3,5,6,7].

So far there was not much interest in Eu-activated BaHfO<sub>3</sub>. Emission of Eu<sup>3+</sup> ion is relatively slow as its f→f transitions are forbidden. Electric dipole induced luminescence of Eu<sup>3+</sup> has usually decay time in the order of 1-1.5 ms and appears when the ion is placed in the site having no inversion symmetry. Magnetic dipole transitions, observed only when Eu<sup>3+</sup> occupies a centrosymmetric site, produce emissions with even longer decay, typically above 4 ms. Such a long luminescence is not appropriate for dynamic medical imaging but is quite ac-

ceptable for planar imaging, also in its digital version with electronic recording of the signal from the phosphor [14].

In this paper we concentrate on structural and spectroscopic characterization of Eu-activated BaHfO<sub>3</sub> prepared in the oxidizing atmosphere of air. One of the issues we will try to elucidate is whether the dopant tends to replace Ba<sup>2+</sup> or Hf<sup>4+</sup> ions, which is further connected with possible charge compensation schemes, quite numerous in every case. Moreover, the possibility of (Eu<sub>Hf</sub> - Eu<sub>Ba</sub>) pair formation should not be overlooked, as such a pair would not require any additional structural defects to balance the incompatibility of the 3+ charge of the dopant ion and the 2+ and 4+ charges of the sites offered by the host.

## Materials and methods

Barium hafnate (BaHfO<sub>3</sub>) powders with the concentration of europium varying in the range of 0-10 at.% were prepared using ceramic method with BaCO<sub>3</sub> (>99%), HfO<sub>2</sub> (99.9%), and Eu<sub>2</sub>O<sub>3</sub> (99.99%) as substrates. It was arbitrary assumed that Eu substitutes Hf in the host lattice and all calculations were performed accordingly. The starting materials were mixed and ground in an alumina mortar with acetone as a wetting medium. After drying the mixture was heated in air at 1400°C for 4h. Following cooling the material was again pulverized by additional grinding and re-heated at the same conditions. To find the best temperature of synthesis a separate series of powders containing 1% of Eu was prepared at different temperatures in the range of 1000-1700 °C.

The X-ray diffraction (XRD) patterns were measured with IRYS diffractometer using Cu K<sub>α1</sub> radiation ( $\lambda = 1.54056 \text{ \AA}$ ) in the range of  $2\theta = 10 - 120$  degree with the step  $\Delta\theta = 0.05^\circ$ . High resolution XRD spectra were recorded with the step  $\Delta\theta = 0.01^\circ$  for the most intensive diffraction lines located around 30.3°, 43.3° and 53.7° to monitor their detailed positions as a function of Eu concentration. Photoluminescence and excitation spectra as well as decay kinetics were recorded using FSL 920 spectrofluorimeter from Edinburgh Instruments. Experiments were performed at room and liquid nitrogen temperature (RT and LN<sub>2</sub>, respectively). Photoluminescence and excitation spectra were taken with a 0.25 nm (RT) and 0.1 nm (LN<sub>2</sub>) resolution. The latter were corrected for the incident light intensity. The RT survey excitation spectrum was recorded with the emission monochromator slits set to 3 nm. For excitation spectra recorded at LN<sub>2</sub> temperature this parameter was set to 0.2 nm which allowed for semi site selective analysis. Decay kinetics measurements were performed using the instrument dedicated Xe flash lamp (60 W) as an excitation source. For these experiments excitation and emission monochromators slits were set to 0.2 nm.

## Structural analysis

Seeking the optimal conditions of the materials preparation we performed synthesis of a series of samples BaHfO<sub>3</sub>:Eu(1%) at different temperatures in the range of 1000-1700°C and monitored the variations in XRD patterns. The results are presented in figure 1. While for all samples the main structural phase was that of cubic BaHfO<sub>3</sub>, only for materials synthesized in the range of temperatures of 1200-1400°C no foreign lines were detected [8,9]. Basing on these results, for further analysis we decided to synthesize all materials at 1400°C. Figure 2a shows X-rays diffraction spectra for BaHfO<sub>3</sub> powders with different concentration of the activator. Independently on the Eu<sup>3+</sup> ion content the XRD patterns do not contain any

cubic  $\text{BaHfO}_3$ -irrelevant diffraction lines, which proves that up to the concentration of 10% Eu dissolves in the barium hafnate host lattice and does not lead to another structural phase.

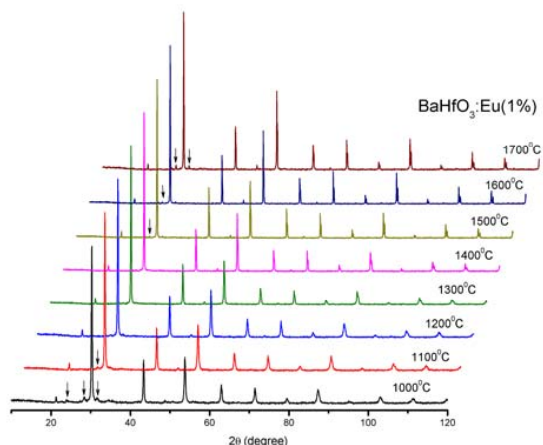


Figure 1. X-ray diffraction patterns for  $\text{BaHfO}_3\text{:Eu}(1\%)$  powders prepared at different temperatures. Arrows indicate lines of unidentified foreign phases.

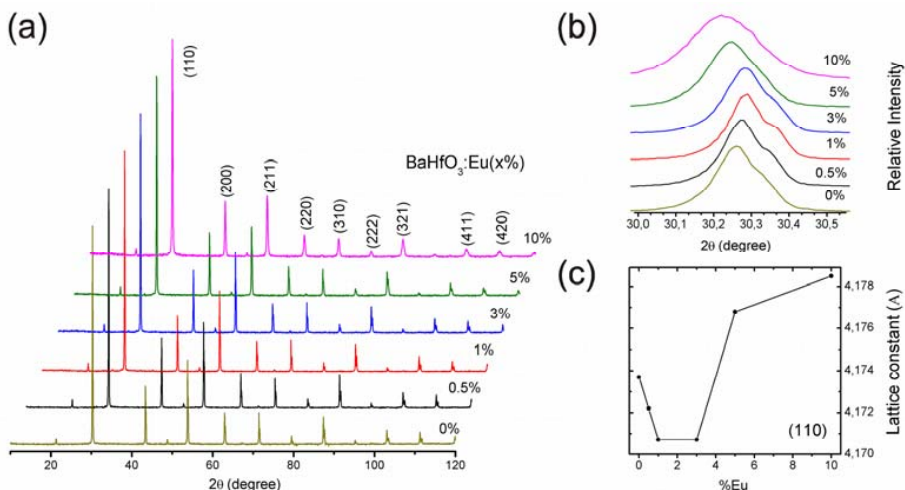


Figure 2. a) XRD patterns for  $\text{BaHfO}_3$  powders with different content of Eu, b) variation in the position of the (110) diffraction line of  $\text{BaHfO}_3\text{:Eu}(x\%)$  powders, c) relation between the cubic lattice constant and concentration of the  $\text{Eu}^{3+}$  ion in  $\text{BaHfO}_3$ .

Figure 2b presents high resolution X-rays diffraction spectra for powders with different content of Eu in the range of angles where the most significant diffraction line appears. Results for other strong lines are very similar. It is immediately seen that the position of the diffraction line shifts to higher angles for the Eu content in the range of 0-3% and goes back to

smaller angles in the range of 3-10% of Eu. Clearly, the Vegard's law [10] is not obeyed in that case. Even more, it looks that contrary processes occur for lower Eu concentrations (0-3%) and for higher Eu contents (5-10%). The changes in position of diffraction lines reflect variations in the size of the unit cell. Figure 2c shows how the perovskite cubic unit cell constant changes with concentration of Eu raising from 0% up to 10%. Clearly, up to 3% the unit cell shrinks and for heavier doping it again expands.

Comparison of ionic radii of  $\text{Eu}^{3+}$  (0.947 Å),  $\text{Ba}^{2+}$  (1.61 Å) and  $\text{Hf}^{4+}$  (0.71 Å) [11] indicates that introduction of the Eu dopant into the barium hafnate varies the unit cell size due to significant differences in the size of the relevant ions. However, from the simple comparison of the sizes we cannot definitely judge about what should happen with the size of the unit cell when  $\text{Eu}^{3+}$  replaces  $\text{Ba}^{2+}$  and what would occur when the dopant goes to the positions of  $\text{Hf}^{4+}$ . We have to be aware that whichever of the two cases happen charge compensation will be required. Consequently, quite a few different possibilities can be anticipated. Below, using the Kröger-Vink notation [12,13], we present only those which seems to be the most probable: (1)  $2\text{Eu}_{\text{Ba}} + \text{O}_i''$ , (2)  $2\text{Eu}_{\text{Ba}} + \text{V}_{\text{Ba}}''$ , (3)  $2\text{Eu}_{\text{Hf}} + \text{V}_{\text{O}}''$ , (4)  $2\text{Eu}_{\text{Hf}} + \text{Ba}_i''$ . Yet, we cannot ignore the option of (5)  $(\text{Eu}_{\text{Ba}} - \text{Eu}_{\text{Hf}})$  pair formation, which would need no additional charge-compensating defect as we already mentioned in introduction.

Analyzing the various possibilities we can easily realize that from the variation of the unit cell size, which we found with high resolution XRD experiments, we cannot undeniably conclude which of the two metal sites offered by the host lattice is indeed entered by  $\text{Eu}^{3+}$  ion. However, from the different changes of the unit cell size for lower range of Eu concentrations compared to the higher Eu contents we can anticipate that the dopant may preferentially enter one of the two sites when the concentrations are low (up to 3%) and the other one when they are higher (above 3%). Consequently, by inference we can further conclude that  $\text{Eu}^{3+}$  enters the  $\text{BaHfO}_3$  lattice substituting both  $\text{Ba}^{2+}$  and  $\text{Hf}^{4+}$ , although presumably with opposite preferences for low and high total Eu concentrations. This in turn would give the ratio of the populations of the two sites,  $\text{Eu}_{\text{Ba}}$  and  $\text{Eu}_{\text{Hf}}$ , dependent on the overall Eu concentration. As we shall see later, further going conclusions will be possible from the spectroscopic data.

## Luminescence spectroscopy

Local positions of  $\text{Ba}^{2+}$  and  $\text{Hf}^{4+}$  ions in the  $\text{BaHfO}_3$  host lattice are centrosymmetric [8]. In the case of the former ion the coordination number is as high as 12 and for the latter one it is 6. If  $\text{Eu}^{3+}$  entering the host preserves the centrosymmetric environment only magnetic dipole induced transitions, with strict selection rules of  $\Delta J = 0, \pm 1$  and  $0 \rightarrow 0$  transition forbidden, would occur in excitation and emission spectra. In the case of  $\text{Eu}^{3+}$  ion basically only  ${}^7\text{F}_0 \rightarrow {}^5\text{D}_1$  in excitation and  ${}^5\text{D}_0 \rightarrow {}^7\text{F}_1$  and  ${}^5\text{D}_1 \rightarrow {}^7\text{F}_{0,1,2}$  in emission spectra would be partially allowed and thus recordable with a standard instrumentation. However, any distortion of the purely centrosymmetric surrounding would relax the selection rules leading to an increase of the number of observed transitions as well as to the rise of their intensities [14,15,16,17].

Figure 3 presents RT excitation and luminescence spectra of  $\text{BaHfO}_3:\text{Eu}(5\%)$ . Emission was recorded upon excitation into the charge transfer (CT) band of  $\text{Eu}^{3+}$  and the excitation spectrum was measured monitoring the 595.6 nm emission with a relatively broad slit (low resolution) of the analyzing monochromator. Hence, these spectra are not site selective. The excitation spectrum consists of a broad CT band peaking around 260 nm and numerous but



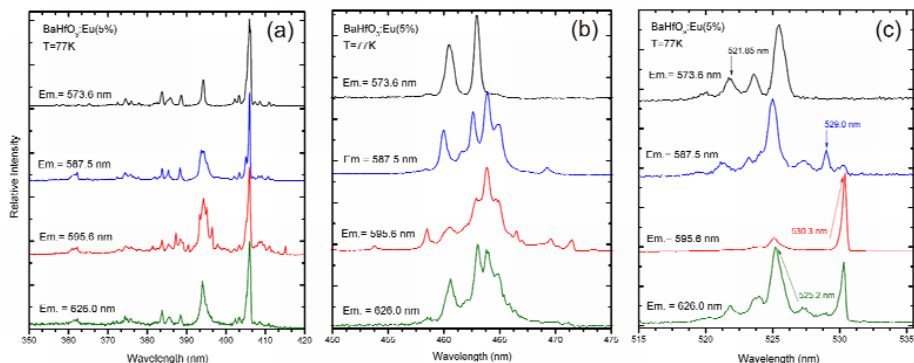


Figure 4. Semi – site – selective excitation spectra of  $\text{BaHfO}_3:\text{Eu}(5\%)$ . The monitored emission wavelengths are indicated in the figure.

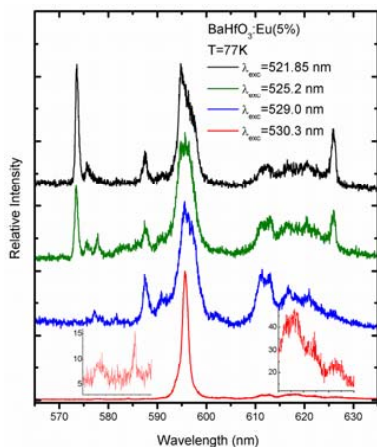


Figure 5. Emission spectra of  $\text{BaHfO}_3:\text{Eu}(5\%)$  upon semi-selective excitation. The stimulation wavelengths are indicated in the figure.

Comparing the excitation spectra it appears clear that they differ significantly attesting the existence of  $\text{Eu}^{3+}$  ions with different symmetry of their local surrounding. Emission spectra obtained upon stimulation of the material into selected excitation lines also differ considerably. All these significant differences could be recorded despite we did not use laser spectroscopy that is we could not excite the different  $\text{Eu}^{3+}$  ions fully selectively. Analysis of the excitation spectra presented in figure 4 allows concluding that at least three of them, for the 573.6 nm, 587.5 nm and 595.6 nm emissions differ in such a way that they have to result from the presence of three different  $\text{Eu}^{3+}$  sites in the  $\text{BaHfO}_3:\text{Eu}(5\%)$  material. Yet, the fourth excitation spectrum of the 626 nm luminescence seems to consist of features already seen in the other three spectra. Indeed, luminescence spectra presented in figure 5 prove that three different emissions, upon excitation with 521.85 nm, 529.0 nm and 530.3 nm radiation, can clearly be distinguished. However, the luminescence excited into the 525.2 nm line

contains only features, which can be found in the other three spectra and therefore cannot be treated as resulting from a separate (fourth)  $\text{Eu}^{3+}$  symmetry site.

An interesting spectral characteristic shows the emission excited with 530.3 nm radiation. Namely, it consists of basically one luminescence line peaking at 595.6 nm. At shorter and longer wavelengths we can find some satellite components but they are of extremely low intensity, and are hardly recordable, indeed. The position of this luminescence indicates that it results from  $^5\text{D}_0 \rightarrow ^7\text{F}_1$  transition and the lack of other components tells to treat this emission as coming from  $\text{Eu}^{3+}$  positioned in a perfectly centrosymmetric site. In the case of the other two  $\text{Eu}^{3+}$  sites, which we identified above, the inversion symmetry has to be broken due to slight distortion because the components which do not come from the magnetic dipole induced transitions show relatively higher intensities.

Since the host lattice offers only two sites for the  $\text{Eu}^{3+}$  ion entering the host, finding three spectroscopically different symmetry sites may be confusing at first. Basing on the presently available results we presume that two of these sites results from the substitution of both  $\text{Ba}^{2+}$  and  $\text{Hf}^{4+}$  ions giving a positively charged  $\text{Eu}_{\text{Ba}}^+$  site and  $\text{Eu}_{\text{Hf}}^-$  site possessing a negative net charge. Since the host does not formally offer a third site for the dopant we hypothesize that the third spectroscopic site of  $\text{Eu}^{3+}$  ion results from the  $(\text{Eu}_{\text{Hf}}^- - \text{Eu}_{\text{Ba}}^+)$  pair formation. To confirm or deny this idea further spectroscopic experiments will have to be performed. We believe that an analysis of a concentration dependence of the luminescence spectra will shed more light on this problem.

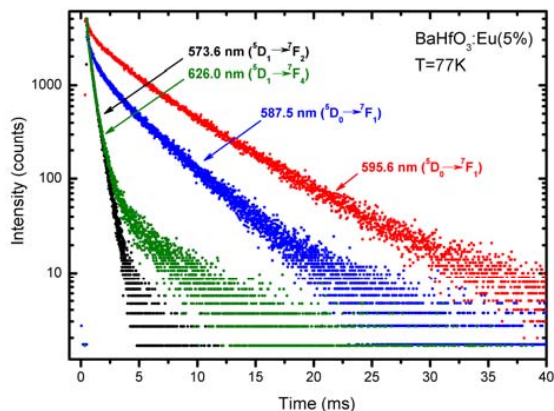


Figure 6. Luminescence decay traces of the main emission lines of the  $\text{BaHfO}_3:\text{Eu}(5\%)$  powder.

To better elucidate the problem of the various luminescent features observed in  $\text{BaHfO}_3:\text{Eu}(5\%)$  powders we recorded the decay traces of the emission lines located at 573.6 nm, 587.5 nm, 595.6 nm and 626.0 nm. The results are presented in figure 6. It is clear that the 573.6 nm and 626.0 nm emissions have common origin. A tail seen in the decay of the 626 nm luminescence results from an overlapping constituent of a longer decay. A closer examination of the energy levels of  $\text{Eu}^{3+}$  tells to assign both this components (573.6 nm and 626.0 nm) to the radiative relaxation of the  $^5\text{D}_1$  level. The decay of the 587.5 nm and 595.6 nm emissions are clearly longer, which is expected as they must necessarily result from a radiative relaxation of the  $^5\text{D}_0$  level of  $\text{Eu}^{3+}$ . The time constants of these two emissions are 3.4 ms

(587.5 nm) and 5.1 ms (595.6 nm), which values are characteristic for  $\text{Eu}^{3+}$  ion in a high-symmetry environment [14,17]. Also, it is reasonable that the value for the 595.6 nm luminescence is longer as we already concluded that this emission results from  $\text{Eu}^{3+}$  ion located in a purely centrosymmetric position. Hence, analysis of the results of XRD measurements, excitation and luminescence spectra as well as decay kinetics leads to quite a consistent picture, with the main conclusion that  $\text{Eu}^{3+}$  ions enters both,  $\text{Ba}^{2+}$  and  $\text{Hf}^{4+}$  positions.

## Conclusions

$\text{Eu}^{3+}$  activated  $\text{BaHfO}_3$  was prepared with ceramic method at 1400 °C. Up to 10 % of Eu content no foreign phase was detected with XRD technique. Results of spectroscopic experiments gave evidence that  $\text{Eu}^{3+}$  ion enters both  $\text{Ba}^{2+}$  and  $\text{Hf}^{4+}$  sites. XRD spectra suggests that the relative population of both sites ( $\text{Eu}_{\text{Hf}}^{\bullet}$  and  $\text{Eu}_{\text{Ba}}^{\bullet}$ ) depends on the overall concentration of Eu. The material containing 5% of the dopant possesses three spectroscopically different sites with clearly different luminescence and excitation spectra. We suppose that the third  $\text{Eu}^{3+}$  site is connected with the formation of ( $\text{Eu}_{\text{Hf}}^{\bullet}$  -  $\text{Eu}_{\text{Ba}}^{\bullet}$ ) pairs.

## References

1. Lambert, P.M., Jarrold, G.S. & Trauernicht, D.P., 1997, US Patent # 5698857.
2. Lambert P.M., Jarrold, G.S. & Bryan P.S., 1998, US Patent # 5786600.
3. Van Loef, E.V., Higgins, W.M., Glodo, J., Brecher, C., Lempicki, A., Venkataramani, V.S., Moses, W.W., Derenzo, S.E. & Shah, K.S., 2007, *IEEE T. Nucl. Sci.* **54** (3), 741.
4. <http://physics.nist.gov/cgi-bin/Xcom/xcom2>
5. Dole, L. & Venkataramani, V.S., 1992, US Patent # 5124072.
6. Venkataramani, V.S., Loureiro, S.M. & Rane, M.V., 2004, US Patent # 6706212 B2.
7. Villanueva-Ibañez, M., Le Luyer, C., Parola, S., Dujardin, C. & Mugnier, J., 2005, *Opt. Mat.*, **27**, 1541.
8. Maekawa, T., Kurosaki, K. & Yamanaka, S., 2006, *J. Alloy Compd.*, **407**, 44.
9. PDF #00-022-0084
10. Denton, A.R. & Ashcroft, N.W., 1991, *Phys. Rev. A*, **43**, 3161.
11. Shannon, R.D., 1976, *Acta Cryst. A*, **32**, 751.
12. Kröger, F.A. & Vink, H.H., 1956, *Solid State Physics*, edited by F. Sietz & D. Turnbull (San Diego, CA: Academic Press).
13. Bridge, F., Davies, G., Robertson, J. & Stoneham, A.M., 1990, *J. Phys.: Condens. Matter*, **2**, 2875.
14. Blasse, G. & Grabmaier, B.C., 1994, *Luminescent Materials* (Springer-Verlag).
15. Derenzo, S.E., Moses, W.W., Weber, M.J., West, Z.C., 1994, *Mater. Res. Soc. Symp. Proc.* **348**, 39.
16. Shionoya, S. & Yen, W.M., 1990, *Phosphors Handbook* (CRC Press LLC).
17. Zych, E., 2002, *J.Phys. : Condens. Mater.*, **14**, 5637.

**Acknowledgements.** The financial support from the Minister of Science and Higher Education under grant # N205 024 31/1207 is greatly acknowledged.